EXPERIMENTATION AT LINEAR e^+e^- COLLIDERS

T.TAUCHI

KEK, National Laboratory for High Energy Physics,
1-1 Oho, Tsukuba, Ibaraki 305, Japan

Recent developments of experimentation at e^+e^- linear colliders are reviewed, which are primarily based on talks presented in the parallel session on Experimentation at this workshop(LCWS95).

1 Introduction

Possibility of e^+e^- linear colliders increases significantly in recent a few years in parallel to this series of international workshops on Physics and Experiments with Linear e^+e^- Colliders. There is a Linear Collider Technical Review Committee(TRC) report [1] on the present status of all linear collider projects in the world together with the experimentation which was presented by Ron Settles in the parallel session on Experimentation. Critical reviews on machine technologies and the experimentation issues are described in the TRC report. All the projects are aiming to produce conceptual designs in next three years.

Issues on experimentation cover a fairly large area, that is experimental scenario, backgrounds, detectors, maintenance of stable collisions between nano-meter beams at interaction point, beam polarization and so on. There were eight talks addressed to the above issues in the session.

In this review, first I will present an experimental scenario for requirements to machine parameters such as center of mass energies and luminosities from a view point of physics interests. The next section is a consideration on backgrounds which are most important issues in the machine interactions. Rather than comparing different approaches in various linear colliders, I will concentrate on a case of JLC [2] for an example of comprehensive study. The detailed comparison can be found in the TRC report. Very recent R/Ds on detectors and positron polarization are also summarized. The last issue is on ground motion and its modeling to provide a stable operation of the machine, which is one of highlights at this workshop. Finally I will summarize the experimentation with future prospects.

2 Experimental Scenario

2.1 Experimentation Phases

There is a rigorous consensus of 500 GeV of e^+e^- center of mass energy at the first phase of linear colliders, which is discussed in the TRC report[1,3] and recent international workshops[4,5]. As shown in Fig.1, the minimum luminosity($\mathcal{L}_{min}$) is well defined as a function of e^+e^- center of mass energy(E_{cm}) by discovery limits of light Higgs(h) and SUSY particles($\tilde{\ell}, \tilde{\chi}^{\pm,0}$), where an integrated luminosity is also indicated as the right vertical axis for one year assuming 10^7 s/year. It can be calculated by

$$\mathcal{L}_{min}^{discovery} = 10^{33} \cdot \left(\frac{E_{cm}}{0.5\mathrm{TeV}}\right)^2 \ \mathrm{cm}^{-2}\mathrm{s}^{-1} \tag{1}$$

,for which ~3,500 events of a process of one unit of R($\equiv$ 87fb/E_{cm}^2(TeV^2)) are created in a year. It should be emphasized that any $\mathcal{SUSY}$ model can be definitely tested at E_{cm} =300GeV, even at E_{cm} =250GeV, since a mass of lightest $\mathcal{SUSY}$-Higgs never exceeds 150GeV [6].

Another superiority of e^+e^- colliders has been proved in testing the standard model of strong and electroweak interactions by precise measurements. Future linear colliders shall proceed to the same business. At the first phase, top quark and gauge boson physics is indeed such subjects in order to determine top quark mass(M_t), its width(Γ_t), α_s, its Yukawa coupling(g_{tth}) and the anomalous couplings of κ, λ, respectively. If ($\mathcal{SUSY}$-)Higgs and $\mathcal{SUSY}$ particles are discovered, linear colliders have to determine their properties in detail, then provide $\mathcal{SUSY}$ parameters of $M_A, \tan\beta, m_0, M, \mu$. In Fig.1 there is another minimum luminosity line corresponding to these precise measurements. It can be expressed by

$$\mathcal{L}_{min}^{precise} = 10^{34} \cdot \frac{E_{cm}}{0.5\mathrm{TeV}} \ \mathrm{cm}^{-2}\mathrm{s}^{-1} \tag{2}$$

,whose dependence of E_{cm} is linear instead of square. Therefore a high luminosity of 10^{34}cm^{-2}s^{-1} or 100 fb^{-1}/year is needed at E_{cm} =500GeV.

There is no doubt that there will be the second phase experiment at higher center of mass energy which is 1TeV at least in order to find a heavy Higgs of ~700GeV if no light Higgs exist. The required luminosity must be $2 \cdot 10^{34}$cm^{-2}s^{-1} or 200 fb^{-1}/year as shown in Fig.1. The minimum luminosity required in this energy region also follows the previous one, that is $\mathcal{L}_{min}^{discovery}(E_{cm})$, for a discovery of new particles such as heavy $\mathcal{SUSY}$ particles in e^+e^- annihilation process. Generally there are many physics interests at the second phase, however they depend strongly on findings at the first

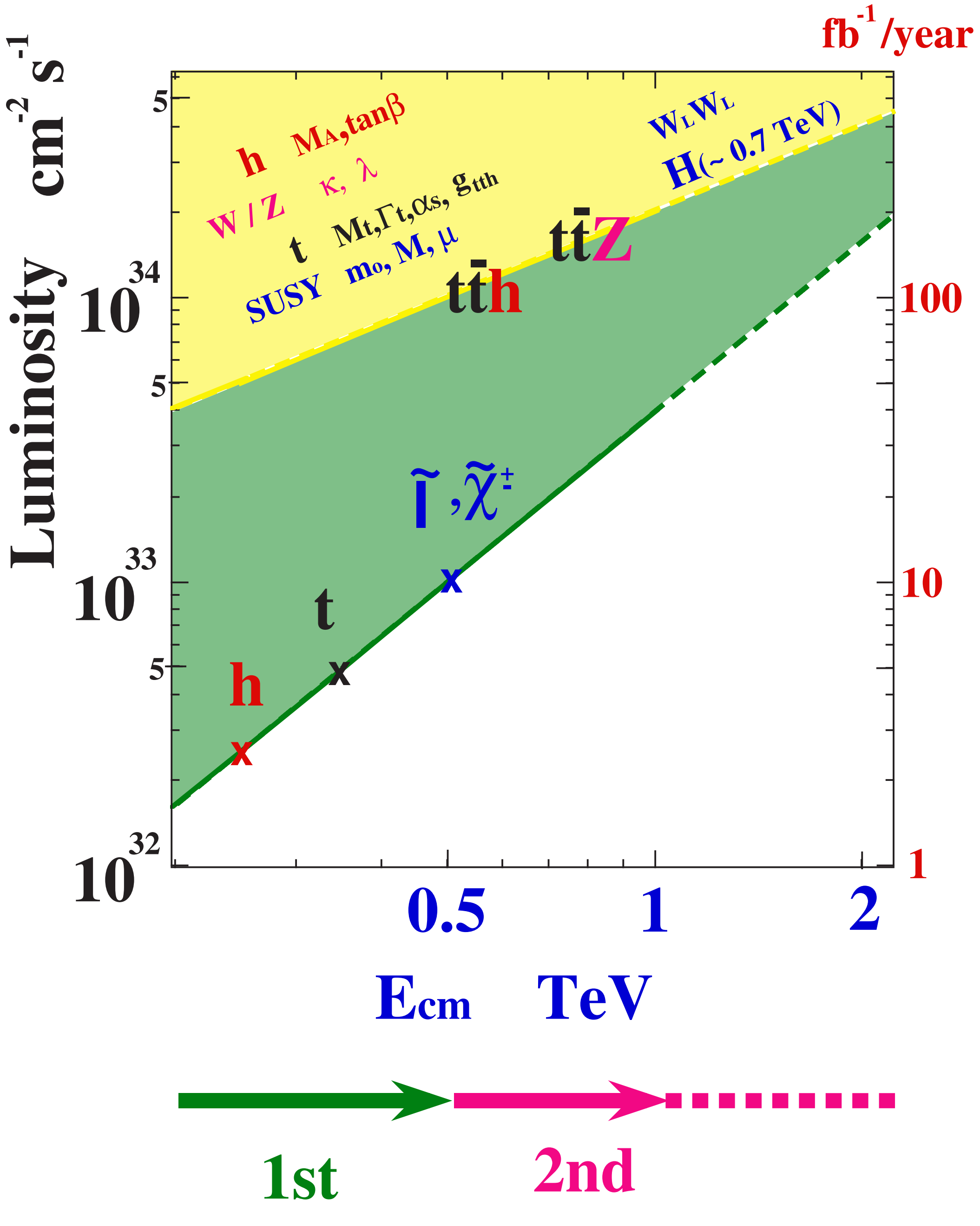

Figure 1: Requirements of luminosity as a function of e^+e^- center of mass energy of linear colliders, where energies of the first and second phases and minimum required luminosities are depicted together with physics targets.

phase. If nature chooses $\mathcal{SUSY}$ scenario beyond the standard model, heavier Higgs and $\mathcal{SUSY}$ particles shall be searched for in order to look into a world of $\mathcal{SUSY}$-GUT. We could also test anomalous interactions with Higgs. If no Higgs exists as a particle, we have to measure a $W_L W_L$ scattering in a world of strongly interacting gauge bosons. At present we do not have a definite answer for the ultimate energy of the second phase to test these possibilities.

2.2 Relation to LHC

An e^+e^- linear collider has been emphasized [8] to be complement to a pp collider under the current schedule that the LHC will have 9.3 TeV collisions in 2004 then full 14 TeV in 2007 [7]. The most relevant complementarity is that 300GeV e^+e^- collider can certainly find a light Higgs boson of $\mathcal{SUSY}$ which the LHC needs ultimate performance to discover since Higgs boson is a key of electroweak symmetry breaking. For full complementarity to pp collider, e^+e^- collider shall operate at optimum center-of-mass energies with high beam polarizations for detailed studies of top quark, Higgs and $\mathcal{SUSY}$ particles as mentioned in the previous section [3].

Since the both colliders have many overlapping regions though in different aspects to explore new physics even at 500GeV e^+e^- linear collider, we should emphasize the competition too for the simultaneous experiments. We have learned from history that healthy competition promoted high energy physics programs in the world and contributed to the understanding of fundamental physics.

3 Backgrounds and Interaction Region Design

In order to see where backgrounds come from, the beam line from the exit of main linear accelerator(linac) to the interaction point(IP) is shown in Fig.2 for JLC-I(E_{cm}) =500GeV [2]. A bending magnet of +20mrad, which is so called big bend, is needed because backgrounds from the upstream linac can not directly hit a detector. The second bending magnet of -16mrad makes a horizontal crossing of $\pm$4mrad between two beams at IP. There are two major sections of 1200m collimation and 600m final focus system in the beam line, where (1)muons and (2)synchrotron radiations are produced, respectively. At IP, (3)e^+e^- pairs and (4)minijets are created in beam-beam interactions. In the subsequent sections these four kinds of backgrounds are briefly discussed together with the possible designs of interaction region against them.

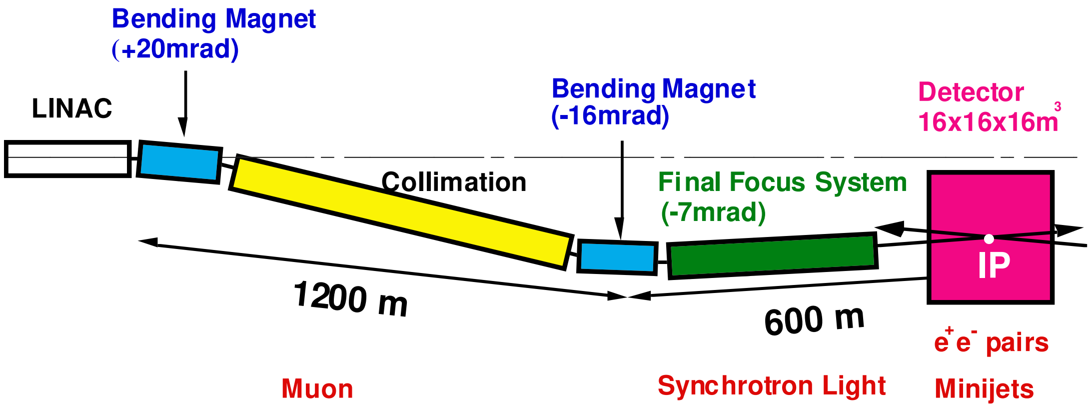

Figure 2: Top-view of a beam line from the exit of main linac to the interaction point (IP) of JLC-I(E_{cm} =500GeV).

3.1 Muons and Collimation

It is expected that transverse profile of beam will not be Gaussian distribution but accompanied by long tail from experience of SLC experiments [9]. While the origin of the tail is not well known at present, we will conservatively assume that beam has a flat tail beyond $3\sigma_{x(y)}$ in horizontal(x) and vertical(y) directions with the relative intensity of 1%. As seen clearly in the next section, beam has to be collimated within $\pm 6\sigma_x$ and $\pm 35\sigma_y$ in order to control backgrounds of synchrotron radiations. Since the real size of beam is order of μm, only the tail must be expanded largely enough for avoiding any destructive deformation of beam by an interaction between the Gaussian core and a collimator, that is non-linear collimation method [2]. This is a reason why 1200m long collimator section is necessary for 250GeV beam. One RF pulse accelerates a train of 85$\sim$50 bunches separating 1.4$\sim$5.6nsec each at 150Hz. As each bunch consists of 10^{10} electrons (or positrons), $10^8 \times 10^2$ electrons will hit collimators at 150Hz.

Two detailed simulations of the muon backgrounds has been made for JLC-I and NLC by Y.Namito and L.Keller [10], respectively. Y.Namito employed a new method of muon attenuator which was originally proposed by E.A.Kushnirenko [11]. The principle idea is to confine μ^+ and μ^- inside two iron pipes magnetized axially in opposite directions and to absorb muons by the energy loss as shown in Fig.3.1. There are four sets of a collimator accompanied by a muon attenuator in the collimator section in order to collimate the horizontal and vertical beam profiles twice for 10^{-8} smearing probability. The best attenuation was obtained to be $10^{-10}\mu/e$ with zero magnetic field in smaller tunnel(R=1.75m) at the furthest collimation point. For NLC,

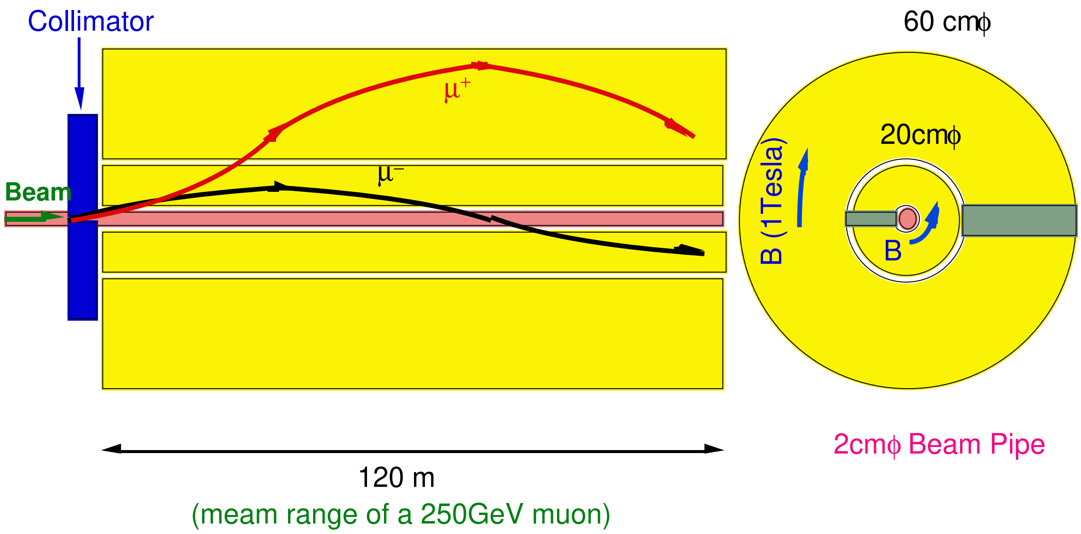

Figure 3: Muon attenuator for JLC-I(KEK) presented by Y.Namito at LC93. Two iron pipes are magnetized axially in opposite directions for both charged muons can be trapped and the 120m length of the iron pipe corresponds to a mean range of 250GeV muons.

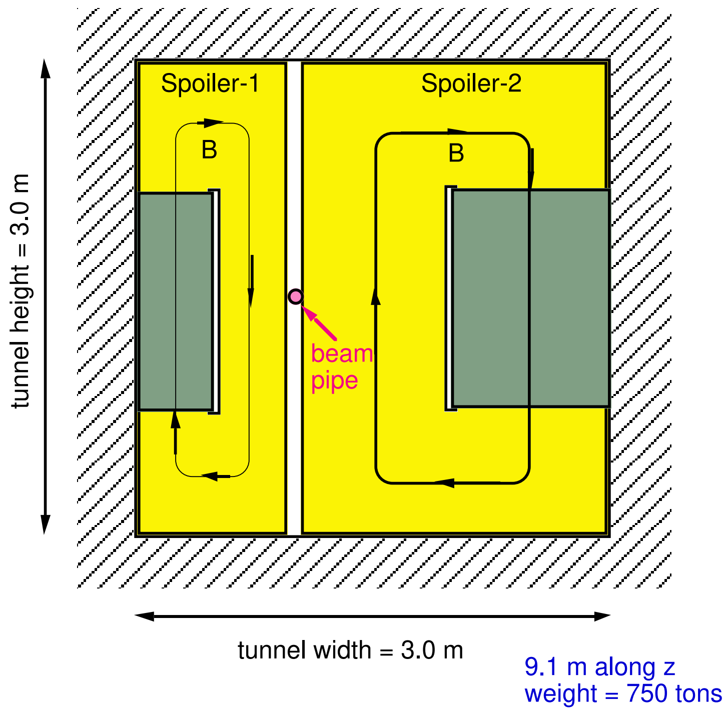

Figure 4: Muon spoiler for NLC(SLAC) presented by L.Keller at LC93. A square tunnel of 3x3m^2 is filled by the 1.5 Tesla magnetized spoiler, whose length and weight are 9.1m and 750 tons, respectively.

L.Keller optimized a system of three and half muon spoilers filling square tunnel of 3x3m^2(Fig.3.1) from valuable experience of SLC experiments, where the half filling spoiler is located inside a big bend and the three are in a final focus system. The result was better than the case of the JLC-I, that is, it can tolerate $10^{10} \sim 10^{11}$ electrons loss per a train corresponding to $10^{-10} \sim 10^{-11}\mu/e$. While more study must be needed on the cost performance and the engineering work, the optimum design would be a combination of the attenuators and the spoilers located at the collimation section and the final focus system, respectively.

3.2 Synchrotron Radiations and Final Focus Quadrupole Magnets

Since the intensity of synchrotron radiations are the same order as a beam itself, it is very dangerous if they scatter at the pole tips of the nearest quadrupole magnet and it is also very difficult to shield them near the IP. The size of synchrotron radiations is determined by the size and divergence of a beam profile since they are emitted tangentially to the beam envelope. The beam size shall be well defined by the collimation, while the divergence is given by the optics($\beta_{x(y)}$) and the emittance($\epsilon_{x(y)}$) in the final focus system with a relation of $\sigma_{\theta_{x(y)}} = \sqrt{\epsilon_{x(y)}/\beta_{x(y)}}$, where $\epsilon_{x(y)} = \sigma_{\theta_{x(y)}} \cdot \sigma_{x(y)}$, to maximize a luminosity. Therefore, the size of synchrotron radiations has to be controlled by the collimation. If we can not control it by all means, we must change the optics to enlarge $\beta_{x(y)}$ so that $\sigma_{\theta_{x(y)}}$ decreases. So we may sacrifice the luminosity. The similar situation likely occurs at the beginning of operation with larger emittance than the expected one as happened in the SLC experiments.

Figure 3.2 shows beam envelops of $6\sigma_x \times 35\sigma_y$ from a last bending magnet to the IP(for a distance of ~140m) at JLC-I, where the smearing effect due to the collimation is not taken account into because its probability was estimated to be very small(10^{-8}). With a mask of 3mm radial aperture located at 60m from the IP, synchrotron radiations from upstream magnets beyond the last bending magnet can be completely collimated so that they pass through the nearest quadrupole magnet(QC1) without scattering, since the half aperture of the QC1 is 6.85mm. As clearly seen in Fig.3.2, the radiations from QC3 and QC2 provide the maximum divergences at the IP in horizontal and vertical directions, respectively. The profiles of the radiations at the QC1 are shown in Fig.3.2. The length and inner aperture of the QC1 are 2.4m and 13.7mmϕ, respectively, and the front face is located at 2.5m from the IP. The in-coming radiations go through a central axis of the QC1. After a collision with 8mrad horizontal crossing angle, the out-going radiations pass at the off-axis, which are depicted as two elliptic profiles connecting each other in Fig.3.2. The both

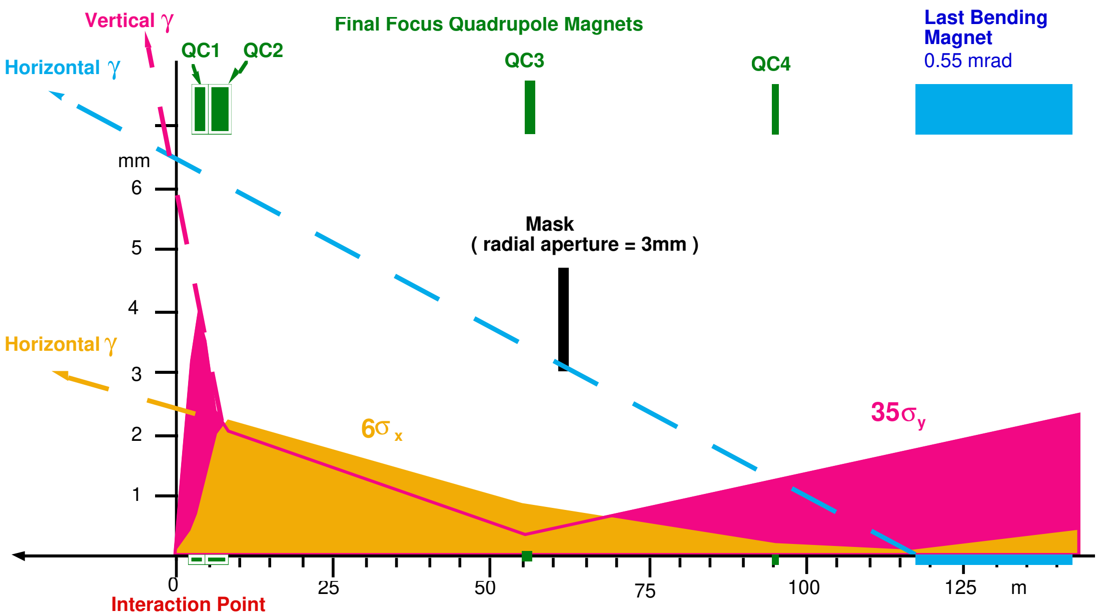

Figure 5: Horizontal($6\sigma_x$) and vertical($35\sigma_x$) beam envelopes through a last bending magnet and four final focus quadrupole magnets(QC1,QC2,QC3,QC4) for JLC-I. Maximum divergences of synchrotron radiations are also drawn by arrows.

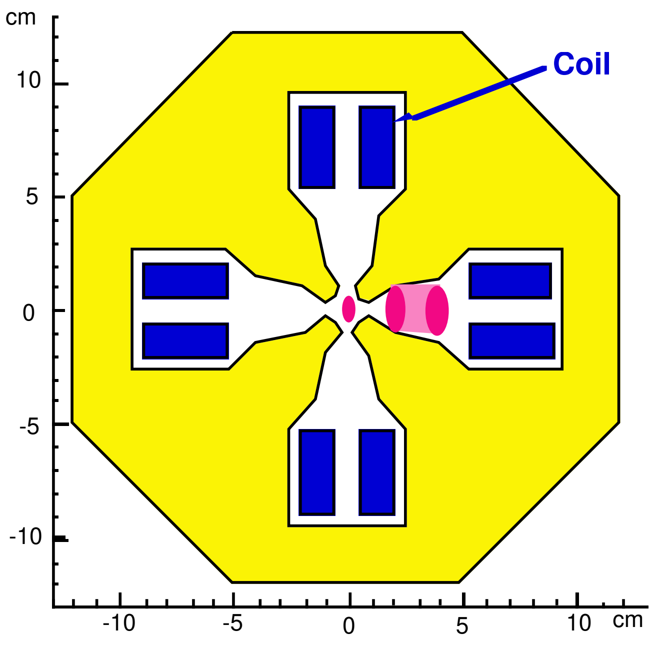

Figure 6: Profiles of synchrotron radiations at the QC1. A profile at the center accompanies the in-coming beam. Two right hand side's ones are passing through the QC1 of 2.4m long after a collision with 8mrad horizontal crossing.

radiations pass through the QC1 without scattering too.

As described above, it is expected that there should be no background problems due to the synchrotron radiations if we carefully optimize the collimation and the optics simultaneously.

3.3 e^+e^- pairs from Beam-beam Interaction and Masking

Enormous amount of e^+e^- pairs will be created during collisions, for instance a few times 10^5 pairs per a bunch crossing at JLC-I. Although most of them are scattered inherently in very forward angles, they can be largely deflected by a strong magnetic field produced by on-coming beam so that they may enter a detector region becoming backgrounds. This process has been studied in details by simulations using ABEL [12] and GUINEA-PIG [13]. Figure 3.3 shows

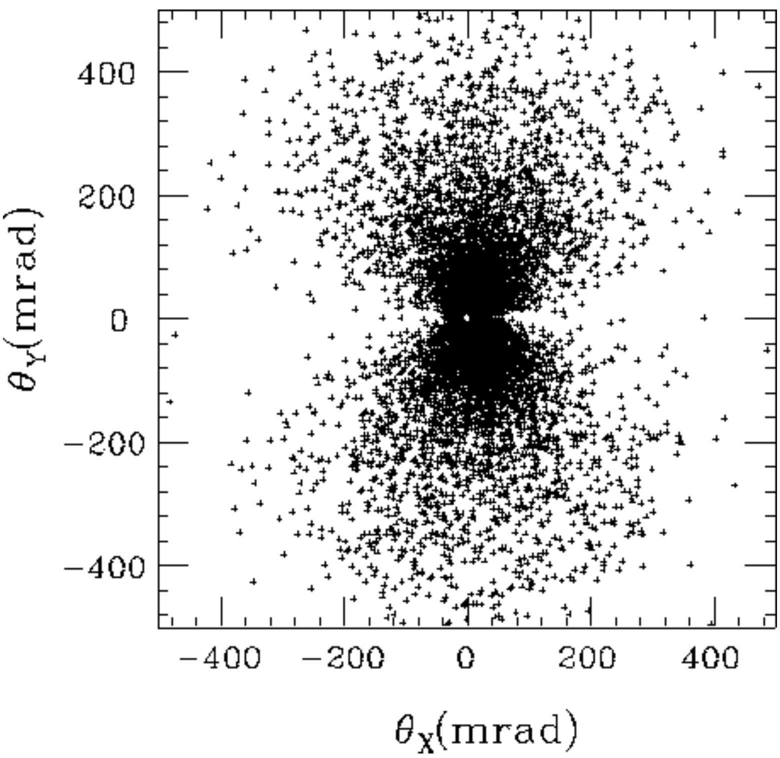

Figure 7: Electrons and positrons scattered by beam-beam interaction at JLC-I, where the the vertical and horizontal axes are the scattering angles in vertical and horizontal directions, respectively.

the angular distributions after the beam-beam interaction obtained by the ABEL for JLC-I. Many particles (electrons or positrons) are scattered in large angle beyond 200mrad. Also we can clearly see asymmetric distribution in the azimuthal direction. More particles are deflected in the vertical direction than the horizontal one because of a very flat transverse beam profile (σ_x^*/σ_y^* = 260nm/3.0nm). Actually a method of measuring nanometer-beam-size has been proposed by using these angular distributions [14]. Since the energies of the particles are relatively small, that is a few hundreds MeV, most of them are confined around a beam axis in a solenoidal magnetic field of 2 Tesla for the case of JLC-I. When they hit the QC1 at the opposite side, a lot of photons are back-scattered uniformly into the detector region to become serious backgrounds.

A masking system has been proposed in order to shield the back-scattered photons as shown in Fig.3.3. A conical mask of heavy metal(tungsten) has been chosen to absorb effectively the photons. The front aperture of the mask was optimized for the core of the particles to pass through the mask. Figure 3.3 shows the radial distribution of the particles as a function of their energies at the front face of the mask, 0.44m from the IP. As clearly seen in the figure, there is the maximum radius of the core, ~5cm, at the energy of 0.1GeV. It is safely smaller than the aperture of 6.7cm. Particles outside the core are scattered inherently in far larger angles than the deflected ones, which are possible backgrounds in the detector to be considered.

In order to numerically estimate the backgrounds due to the pairs in a vertex detector, we plot the number of hits for the particles to traverse a surface of cylinder as a function of its radius assuming no interaction there in Fig.3.3. Remembering that a train consists of 72 bunches in this case(JLC-I(c)), the total number of hits amounts an order of 10^4 per a train crossing, during $\sim$ 200nsec, at R_{vtx}=2cm. In the central tracking region at R_{vtx} >30cm, the total number of hits is expected to be less than 100/train.

Very recently D.Schulte proposed the similar masking system (Fig.11) with more detailed simulations for TESLA at LC95 [15]. He found that back-scattered electrons (positrons) contribute to the hits at the vertex detector more than the primary particles although they would reach the detector more than 20 n seconds later. To reduce them, additional masks are introduced around a superconducting quadrupole magnet and inside the mask as shown in Fig.11. A graphite mask was found to effectively absorb back-scattered particles of lower energies. With this configuration, he calculated the number of hits in the inner layer of the vertex detector at r_{VTX} =15~30mm as a function of half aperture of the inside mask, r_{mask}. In this case, the back-scattered particles were also taken account of by the simulation. As clearly seen in Fig.12, smaller r_{mask} can reduce the number of hits significantly even at r_{VTX} =15mm. Since the bunch separation of TESLA is 1μsec while 1.4-5.8nsec for JLC-I, the resultant hit number can be compared to the numbers per a train crossing for JLC-I.

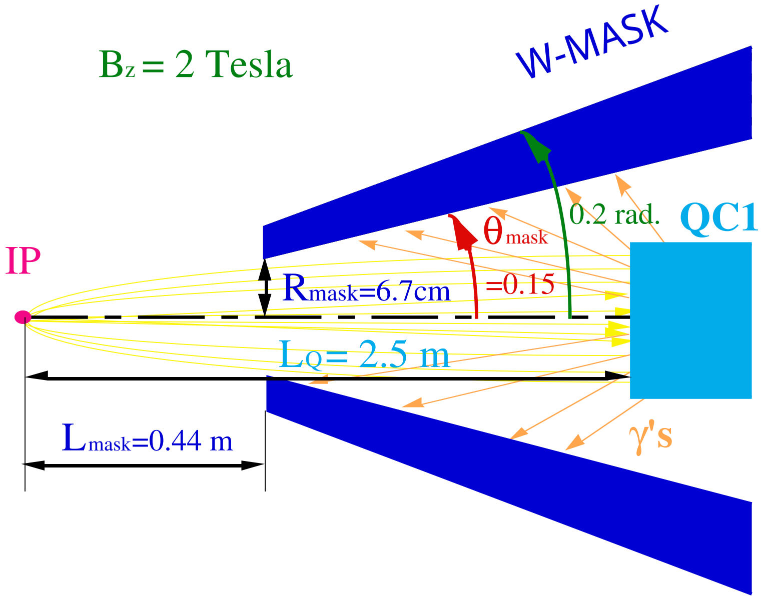

Figure 8: Masking system in a solenoidal magnetic field of 2 Tesla around the IP for JLC-I.

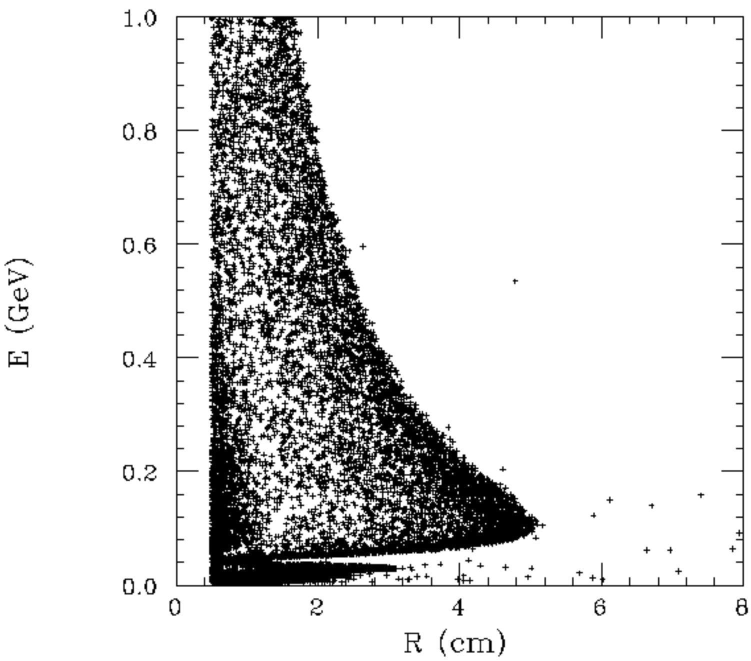

Figure 9: Particles of e^+e^- pairs at the front face of the mask (44cm from the IP) for JLC-I, where the vertical axis is their energy and the horizontal one is their radial position.

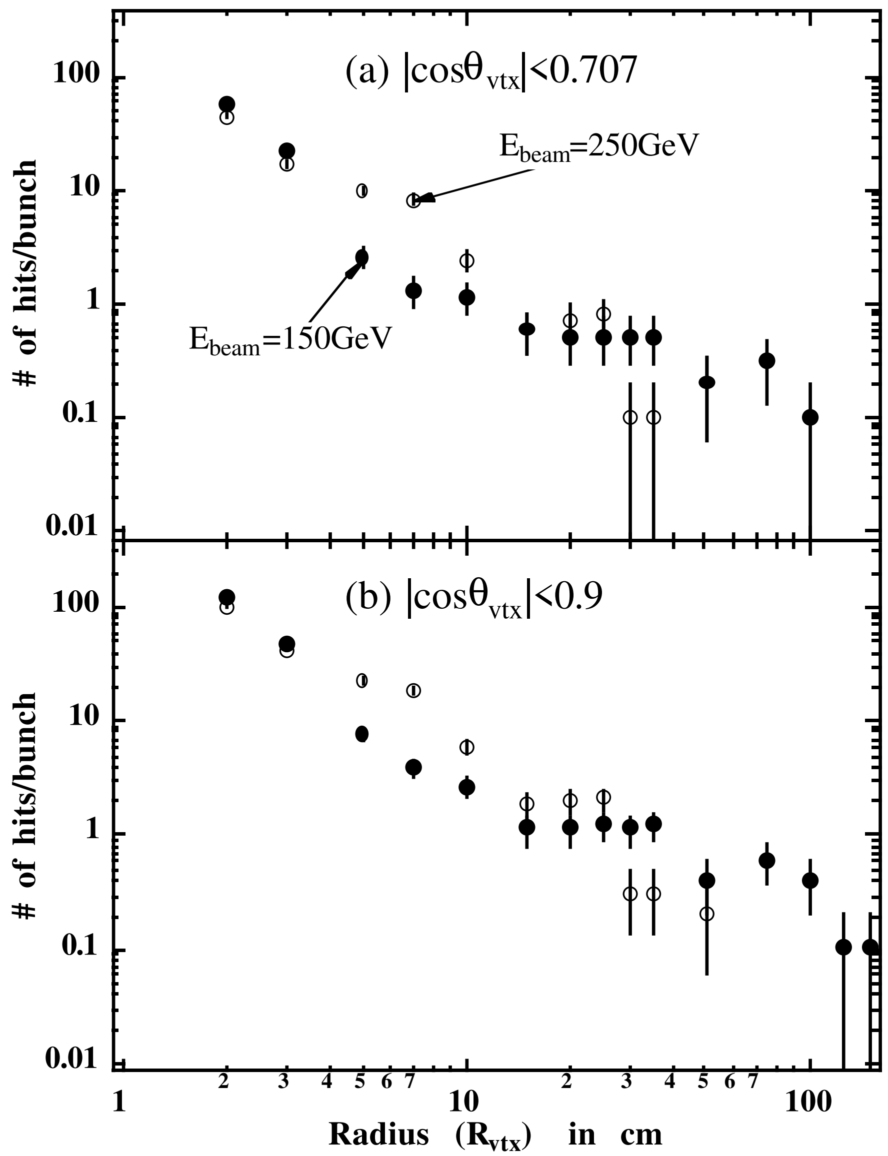

Figure 10: Hits per a bunch crossing by the pairs in B=2Tesla as a function of radius(R_{vtx} of a cylinder for two angular regions of (a) and (b) for JLC-I.

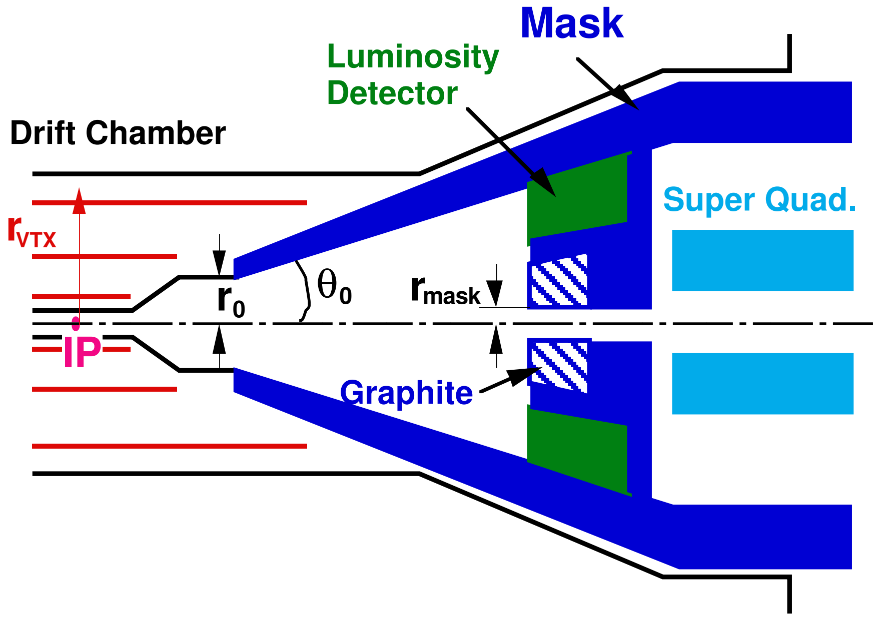

Figure 11: Masking system for TESLA proposed by D.Schulte at LC95, where θ_0 =66mrad and r_0 =33mm. The nearest superconducting quadrupole magnet is located at 3m from the IP, and the aperture is 48mmϕ.

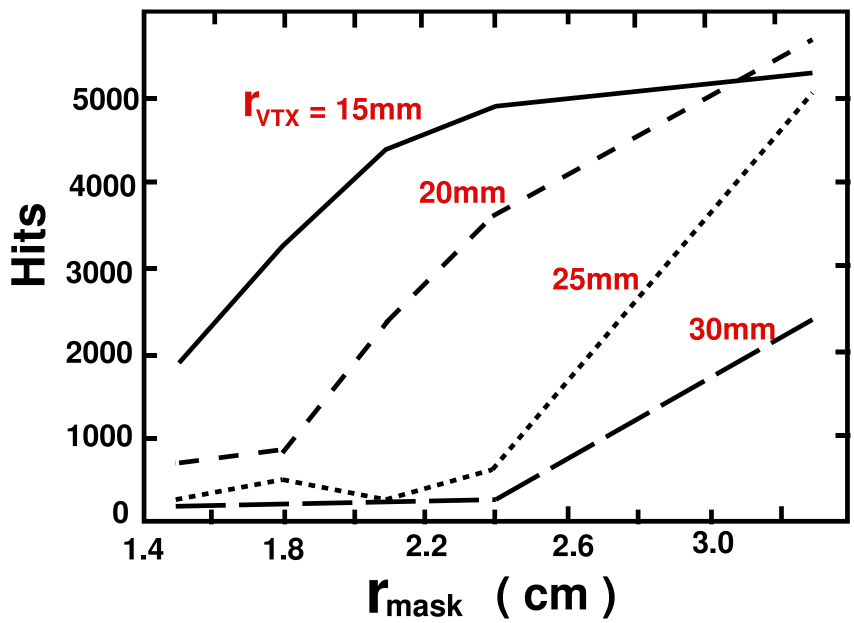

Figure 12: Hits per a bunch crossing in the inner layer of the vertex detector for TESLA, where the vertex detector covers the angular region of θ >200mrad.

3.4 Minijets

Hadronic backgrounds, so called minijets, have been estimated for proposed linear colliders at recent workshops [16,10,4,5]. Since the calculations depend on the poorly known gluon content of a photon at small Feynman x value of less than 0.1, they have a large ambiguity, for instance more than 100%. For the comparison between various linear colliders, the method of P.Chen et.al.[17] has been employed as the standard calculation in the TRC report.[a] According to the report, the numbers of minijets are 0.0052 and 0.0032 per a bunch crossing for JLC-I(c) and TESLA, respectively, with p_T^{min} = 3.2GeV and $E_{\gamma\gamma}$ >5GeV, while the hadronic events of $E_{\gamma\gamma}$ >5GeV are 3 and 5 times more than the minijets. Since the rates are still low and also the events are boosted in very forward angular region, no serious problem is expected at E_{cm} =500GeV at least.

4 Detector

The parameters of the JLC detector has not been changed since the green book[2],1992. The primary goals are (1) hermetic calorimetry covering $|\cos\theta|$ <0.98 located inside the magnet coil of 2 Tesla solenoidal field, (2) high precision tracking to reconstruct a recoil mass of light Higgs boson with the resolution of ~200MeV in the process of $e^+e^- \to hZ,\ Z \to \ell^+\ell^-,\ h \to$ anything, and (3) good vertexing to detect b-quarks in many backgrounds. The technique has been chosen to be conventional so that the scale of the JLC detector is large as shown in Fig.13.

Recently European group proposed the "1 TeV detector" [3] as a high performance detector, which is very similar to the JLC. A detector with higher magnetic field (4 Tesla) has been suggested to optimize the performance of vertexing (next section) by C.Damerell at the previous workshop. Such an alternative detector shall be considered seriously too.

4.1 Vertexing

There have been two R&D programs [19,18] on vertex detectors toward experiments at linear colliders, both of which are based on Charge-Coupled Devices(CCDs).

The JLC group has been concentrated on the CCD of 25μm pixel operating in a room temperature($>$ 0°C) with good radiation hardness, although the existing device(SLD-CCD) is set in a cryostat of −83°C as the other program.

[a]Actually the method was improved to include the direct and once-resolved processes with the GUINEA-PIG's calculation of beamstrahlung photons by D.Schulte.

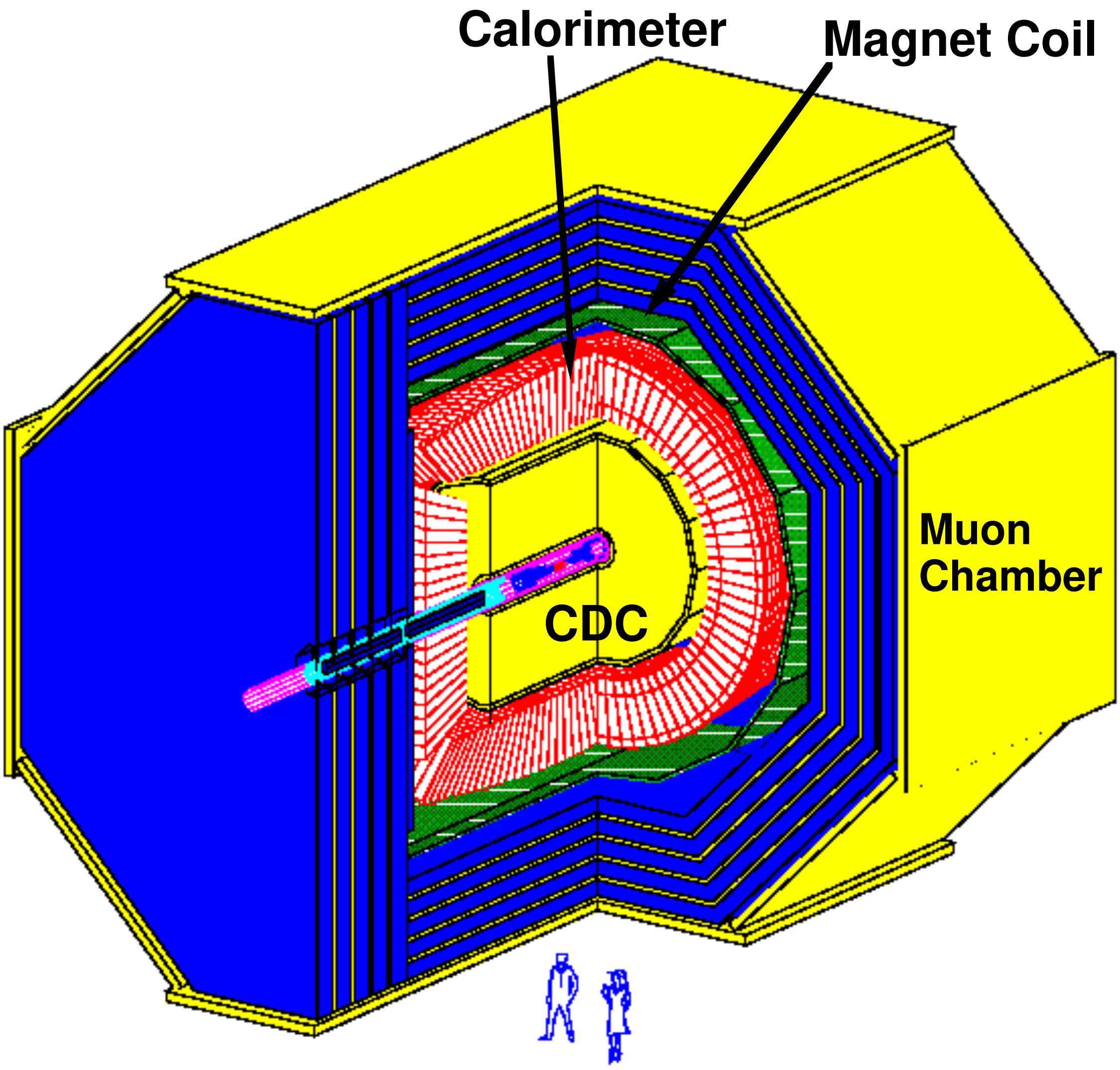

Figure 13: Schematic view of the JLC detector. The total volume and weight are $16 \times 16 \times 16\mathrm{m}^3$ and 15,000 ton, respectively.

The main R&D items are to use a silicon-wafer with higher resitivity($\sim$1kΩ cm) and the thicker depletion region($\sim$30μm) in order to improve the S/N ratio. The shot noise(σ_{dark}) has been measured to be 40 e(electrons) in 0°C at the readout frequency of 63kHz, so it is expected to be 10e at 1MHz [21,20]. Since a minimum ionizing particle (MIP) creates about 1,200 e, that is σ_{MIP} =35e, it fills the principle requirement if it is operated in 0°C. The next will be a test of the radiation hardness.

C.Damerell suggested the ultimate performance for future linear colliders based on the experience of the SLD-CCD detector which is the first full custom design for high energy experiments [18]. The performance and some requirements are listed in Tab.1. In order to put the detector at R$_{min}$=1cm from the beam line, the hit density due to backgrounds must be less than 2/mm^2 per a train crossing there. Since this tolerable limit is already at R$_{min}$=2cm in B=2Tesla for JLC-I as described in 3.3, high solenoid field of 4 Tesla should be needed to control the backgrounds. The thinnest layer configuration of the detector will be provided by a 20μm silicon with a beryllium stiffener. He also speculated for the readout rate to be more than 20MHz in future with a careful design of the readout circuit.

Table 1: The present and future performances of 25μm pixel CCD detectors.

Present (SLD)		Future Linear Collider
$\sigma_{xy} = 11\mu\text{m} \oplus \frac{29\mu\text{m}}{p \cdot \sin^{3/2}\theta}$		$\sigma_{xy} = 3\mu\text{m} \oplus \frac{5.5\mu\text{m}}{p \cdot \sin^{3/2}\theta}$
$\sigma_{RZ} = 18\mu\text{m} \oplus \frac{29\mu\text{m}}{p \cdot \sin^{3/2}\theta}$		$\sigma_{RZ} \approx \sigma_{xy}$
R$_{min}$	3 cm	1cm
X$_0$/layer	0.35%	0.12%
Si/layer	200 μm^t	20 μm^t
β_e/layer	0.38 mm^t	0.38 mm^t

where, σ = (pixel size, R$_{min}$) $\oplus$ (multiple scattering).

D.Jackson cleverly demonstrated the superiority of the SLD-CCD detector by a topological vertex reconstruction [22]. For instance, the SLD obtained τ_{B^+}/τ_{B^0} with better accuracy than the DELPHI, even the SLD has only 10% statistics(hadronic Z decays) of the DELPHI. For future linear colliders, the goal is to reconstruct a primary,secondary and tertiary vertices in order to identify charm and bottom quarks exclusively by the topological method. The bench mark physics would be a measurement of branching ratio of $h \to c\bar{c}$ for the determination of $\mathcal{SUSY}$ parameters [23].

4.2 Tracking

Once a required momentum resolution is determined, the scale of tracking detector is calculated by a well known equation [24] of

$$\sigma_{1/p_t} \equiv \frac{\sigma_{p_t}}{p_t^2} = \frac{\sigma_x}{0.3BL^2}\sqrt{\frac{720}{N+5}} \tag{3}$$

,where p_t, σ_x, L, N and B are transverse momentum (GeV), the spatial resolution(m), length(m) of measuring a trajectory, the number of sampling points and solenoid field(Tesla).

As mentioned before, the JLC group set the momentum resolution from "the recoil mass resolution of light Higgs boson = beam energy spread of 200MeV", that is $\sigma_{1/p_t} = 1 \cdot 10^{-4}$. The L is calculated to be 2m with σ_x =100μm, N =100($\approx L/0.02$) of a conventional drift chamber comprizing small jet-cells and B =2Tesla. The outer radius was turned out to be 2.3m with the inner radius of 0.3m as shown in Fig.13. So the wires are 4.6m long to cover the angular region of $|\cos\theta| < 0.7$ for the full sampling. Because of such long wires, there are R&D issues on the stability of wire tension, the gravitational and electrostatic sags and so on.

N.Khalatyan presented the results of the JLC-CDC test chamber of 30$\times$30cm^2 and 4.6m long comprizing 5 small cells [25]. The tension of all field wires, which are 120μmϕ gold plated aluminum, has been decreased by 10% over a year. The reason was considered to be the material itself because of the uniformly lengthening. So the good material has to be looked for. The gravitational sags were measured to be 355μm and 600μm for the sense wires of 30μmϕ gold plated tungsten and the field wires, respectively. They are in good agreement with the calculations. The electrostatic sag of the sense wires was also measured to be 110μm, which fairly agrees with the calculated value of 85μm. So these sags can be corrected to achieve the designed resolution.

In order to separate background trajectories coming from neighboring bunch crossings, the time resolution must be crucial. If a charged particle hits all 100 wires, the time resolution for the trajectory can be obtained to be 10nsec/$\sqrt{100}$=1nsec because of the drift velocity of 10μm/nsec. Therefore the originating bunch can be identified for the bunch spacing of 1.4$\sim$5.6 nsec for JLC-I.

4.3 Calorimetry

The JLC group has made two kinds of test modules corresponding to one unit of the hadronic part of the calorimeter(Fig.13) as reported at the LCWS93 [4]. The standard calorimeter is a sandwich type of lead and plastic scintillator(SAND), and the second option is a lead/scintillating fiber calorimeter(LESFI). The both are so called compensating calorimeters providing the same energy deposit for electrons and pions(hadrons). At this workshop, K.Ishii presented the results of the beam tests by using 1$\sim$4GeV electron and negative pion beams at KEK [26]. The results are summarized in Tab.2.

Table 2: Beam test results of the test calorimeter modules by 1$\sim$4GeV e^-,π^- beams at KEK. All the test modules have the same cross section of 20$\times$20 cm^2.

$$\sigma/E = A/\sqrt{E} \oplus B\ (\%)$$

for electrons

module		EM structure	A	B
LESFI	173 X_0	1mmϕ fibers in Pb	15.2	-0.6
SAND	29 X_0	2.5mm^t scint., 10mm^t Pb	24.0	1.2
F-SAND	29 X_0	1.0mm^t scint., 4.0mm^t Pb	15.4	0.2

for negative pions

module		HAD structure	A	B
LESFI	6.2 λ	1mmϕ fibers in Pb	30.1	7.5
SAND	6.5 $\lambda^{a)}$	2.0mm^t scint., 8mm^t Pb	41.9	7.7

a) 6.5 λ is the total absorption length with the electromagnetic part(EM).

For electrons, the LESFI and the fine sampling (F-)SAND fulfill the required energy resolutions including the constant term. For pions, the large constant terms(B$\sim$8%) were observed in the both modules. The cause was speculated to be the lateral shower leakage, which will be checked by a beam test.

In order to readout the signals in 2Tesla solenoid field, three kinds of devices, fine mesh photomultiplier(FMPMT), hybrid photo-diode(HPD) and vacuum avalanche photo-diode(VAPD), were also tested in a magnetic field up to 2.5Tesla. While the FMPMT and the HPD were operational even in 2.5Tesla, the HPD seems to be better because of the stable gains in B=0$\sim$2.5Tesla and the uniform response for any direction of the magnetic field. Although the present readout uses wavelength shifters, a CDF type tile/fiber readout [27] will be considered in future for no gap between modules.

5 Positron Polarization

A physics potential adding positron polarization has recently been demonstrated in a precise measurement of $\sin^2\theta_W$ on Z-pole [28]. With $P_{e^-} = -90\%$ and $P_{e^+} = -80\%$, the systematic error($\Delta\sin^2\theta_W$)can be 5 times smaller than that of single polarization($P_{e^-} = -90\%$), that is $\Delta\sin^2\theta_W = \pm 0.00005$. This accuracy would significantly constrain the mass of heavy Higgs bosons if the first phase collider could not find a Higgs boson. In addition, a new physics signal can be ambiguously measured in the initial states of $e^+_L e^-_L$ and $e^+_R e^-_R$ for hardly interacting in the standard model. For instant a process of $e^+_R e^-_R \rightarrow \tilde{e}^-_R \tilde{\chi}^+ \bar{\nu}$ can be observed with no SM background [29].

T.Hirose described the R&D program and the present status of polarized positrons [30]. The two methods have been considered as follows. The first is to use β^+ decay of unstable nucleus, that is $^{27}Si \rightarrow {}^{27}Al + e^+ + \nu_e$ where ^{27}Si is made in process of $p + {}^{27}Al \rightarrow {}^{27}Si + n$ by protons bombarding aluminum plate. The present setup is based on the commercial proton cyclotron, CYPRIS of Sumitomo Heavy Industries Ltd., which accelerates protons up to 18MeV with the beam intensity of 1μA. The positrons from the β^+ decay must be monochromized energetically in a moderator of 25μm^t tungsten plate, then they will be accelerated. The present intensity of positrons is expected to be 4.3×10^5/sec for the polarization of more than 80% with 10^{-4} efficiency(ϵ) of the moderator. The first mile stone of the R&D is to measure the actual intensity and polarization of positrons. In order to fulfill the requirement of $10^{14}e^+$/sec for the JLC-I, 40MeV proton beams of 100mA are needed in addition to the dramatic improvement of the efficiency of moderator, $\epsilon = 0.2$.

The second method is to use e^+e^- pair creations by polarized photons which are back-scattered from Compton scatterings between circularly polarized laser lights and high energy electrons. The test experiment is conducting by using 1.5 GeV e^- beams of ATF-linac at KEK. The beam of $2\times10^{10}e^-$/bunch collides with 2.33 eV YAG laser beam of 0.55J/pulse to produce polarized photons(<80MeV) of $4.4\times10^5\gamma$/bunch. Polarized positrons (>80%) are expected to be created with the intensity of 1.4×10^4/bunch from 3mm$t$ tungsten target hit by the photons[31]. For the JLC-I, high intensity 5GeV linac of more than $10^{12}e^-$/bunch is needed together with a multi-converter system comprizing $\sim$100(number of bunches) CO_2 lasers of 5J/500ps which are operational at 150Hz and are driven by a Nd:YAG laser to precisely control their timings. The different methods have recently been proposed to produce high energy polarized photons emitted in undulators at 100$\sim$200 GeV e^- linac and at a relativistic ion storage ring for more efficient source of polarized positrons [32].

Although a lot of R&D and breakthrough must be necessary to realize the polarized positron beam, it is worth to pursue it.

6 Ground Motions

Since the vertical beam size is a few nanometer at IP for future linear colliders, the ground motion must be understood quantitatively as a function of the frequency(ω) and the wave number(k). For this purpose,it has recently been proposed that measurements at many different places could be expressed universally by a simple formula, so called ATL rule[33]. That is, a time variance of relative displacement(Δy) between two points can be expressed by

$$< \Delta y^2 >= A \cdot T \cdot L \tag{4}$$

,where A (m^2/sec/m) is a coefficient depending on various places, T(sec) is the time interval of measurements, and L(m) is the distance between the two. The simple application is the vertical ground motion between two nearest quadrupole magnets, which are separated by 5m(=L) for JLC-I, assuming that a fast feedback can be effective at the frequency of less than 10Hz, so T=0.1sec for the minimum time interval. Table 3 lists the calculations for three different

Table 3: Vertical ground motions estimated by the ATL rule at various places, assuming the distance of L=5m and the time interval of T=0.1sec.

place	A (m^2/sec/m)	$< \Delta y^2 >^{1/2}$ (nm)
KEK	$2 \cdot 10^{-16}$	10
HERA	$3 \cdot 10^{-17}$	3.9
Sazare	$1 \cdot 10^{-18}$	0.7

places; KEK, HERA and Sazare which is an old mine at mountain-side tunnel in Shikoku island, Japan. The nanometer beams pass each other except for Sazare if there is no coherent movement between the two magnets. So these calculations conclude that the rigid support system is definitely necessary [34]. Although this estimation is too simplified, we can see clearly how the ground motion affects the final focus magnets.

S.Takeda (M.Yoshioka) presented the ground motions measured at four places, which are Sakurajima(volcanic), Sazare(green schist), ATF-KEK(solid clay) and Esashi(Granite) from south to north, in Japan, at the wide frequency region from 10^{-7} to 100Hz[35]. Some of the results are shown in Fig.6 compared to various places in the world. Peaks seen around 0.2Hz are due to ocean waves, while a peak at 3Hz observed at ATF-night is a resonance of the earth's crust probably by the traffic around. At ATF, the day movements were much larger than the night ones at 0.1$\sim$10 Hz, for instance 10,000 times at 1Hz. This implies that cultural noises must be seriously considered and they are dominant in real life. In addition, micro earthquakes have been observed at ATF, whose magnitude is comparable to the day motion. It should be also noted that there are two clusters in the power spectra at the frequency of >10Hz, where the motions of surface grounds(ATF,Sazare,SLC and CERN-TT2A) are larger by an order magnitude than those of deep undergrounds(LEP and UNK tunnels).

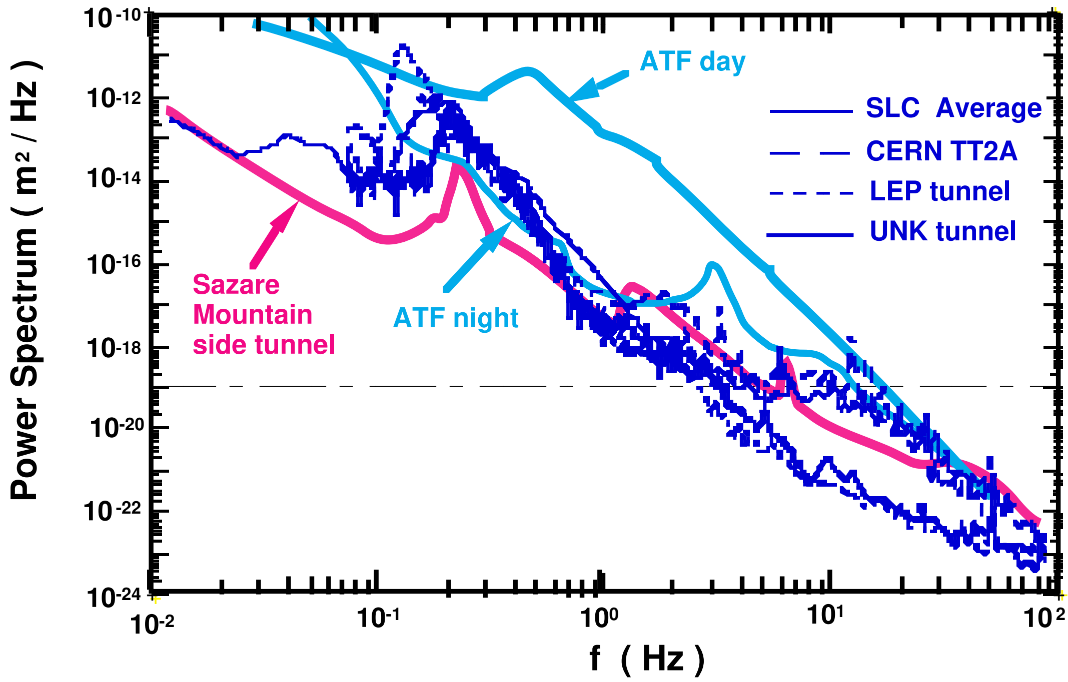

Figure 14: Power spectrum density of vertical ground motion at various places.

C.Adolphsen had a very impressive talk on ground motion tolerances based on measurements in the SLC linac tunnel by building a ground motion model[36]. It has been emphasized that the stability of nanometer beam collisions can be estimated accurately if we know the two dimensional(ω, k) power spectrum of the ground motion at the site of linear collider. Vertical ground motions have been measured simultaneously at 9 points located at 0, 2, 24, 50, 100,200, 400, 988, 2000m in the SLC tunnel. The data were recorded for 1.8 hours scanning at 128Hz effectively. After the Fourier analysis, all the data were well fitted by a model of two dimensional plane wave propagating on the surface of the ground with the phase velocities depending on the frequencies. Convoluting with the optics in two linacs, they calculated the r.m.s. beam separation(Δy_{IP}) due to the ground motions in the linacs at IP, then its Fourier components too. Finally they estimated the ground motion tolerances as a function of the frequency as shown in Fig.15. Comparing to the tolerance with the feedback of the SLC type which is apparently effective at the frequency of <3 Hz, the effect of the ground motions is turned out to be tolerable in the SLC tunnel.

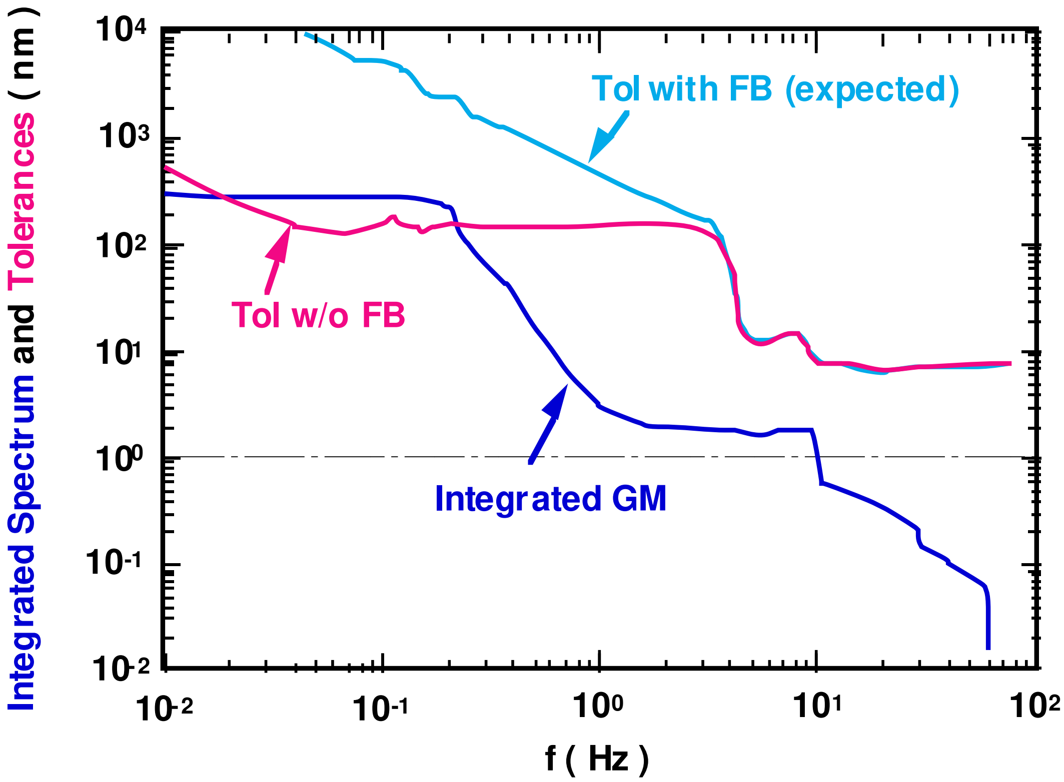

Figure 15: Ground motion tolerances and integrated spectrum as a function of frequency, based on SLC linac measurements during "quiet" conditions.

7 Summary

The experimental scenario comprizes two phases of linear colliders. The first phase is well defined at E_{cm} =500GeV. The maximum energy of the second phase is slightly obscure, probably $E_{cm} = 1 \sim 2$TeV, which must be further investigated although it depends on findings at the first phase. The competition with the LHC should be emphasized as well as the complementarity for the simultaneous experiments and the healthy program of high energy physics.

All the backgrounds are under control so that we can optimize the linac parameters together with the detector designs. The detailed simulations would be needed for each linear collider including detectors.

Vertexing based on the CCD has been proved to be promising. The three dimensional topological method could clearly reconstruct primary, secondary and tertiary vertices to identify u,d,s,c,b and t quarks ultimately. The active R$Ds on tracking and calorimetry have been also conducting for the JLC-I. New ideas shall be called for a compact detector, high magnetic field and particle identification and so on. We expect that a lot of benefits must come from R&Ds of the LHC detectors.

A new R&D of polarized positron beams has been initiated in Japan. This effort should be encouraged in order to significantly strengthen the physics potential for the full ability of linear colliders.

There were very nice two dimensional measurements of ground motions and the modeling at SLAC. It was demonstrated that the ground motions were also under control. Seriousness of culture noises and micro-earthquake was emphasized. Resultantly more works are needed on a fast feedback in linacs, a support system at the interaction region, and also a consideration of deep underground site for linear colliders.

So we expected more R&Ds for next few years towards conceptual designs of linear colliders.

Acknowledgments

I would like to thank conveners of the experimentation session, R.Jacobsen, S.-K.Kim and R.Settles for well organized session. I appreciate stimulated discussions with R.Settles, T.Hirose, C.Adolphsen, M.Yoshioka, S.Takeda, C.Damerell, D.Jackson, N.Khalatyan and K.Ishii. This work was supported in part by JSPS Japanese-German Cooperative Program.

References

1. G.Loew, these proceedings, and *Linear Collider Technical Review Committee Report 1995* to be published.
2. JLC group, JLC-I(the green book),*KEK Report* 92-16, 1992.
3. R.Settles, these proceedings, and also in the TRC report [1].
4. Proceedings of Workshop on *Physics and Experiments with Linear e^+e^- Colliders(LCWS93)*, eds. F.A.Harris, S.L.Olsen, S.Pakvasa and X.Tata (World Scientific, Singapore, 1993).
5. Proceedings of *Sixth International Workshop on Linear Colliders (LC95)*, ed. J.Urakawa, *KEK Proceedings* 95-5, August 1995.
6. Y.Okada, these proceedings.
7. Liewellyn-Smith, talk at *17th international Symposium on Lepton-Photon Interactions*,Beijing, China, 7-12 August, 1995.
8. M.E.Peskin,*Complementarity of e^+e^- and pp colliders from the Exploration of Electroweak Symmetry Breaking*, SLAC-PUB-6582, Aug 1994. Lectures given at *22nd INS International Symposium on Physics with High Energy Colliders*, Tokyo, Japan,8-10 Mar 1994.
9. ,D.Burke, proceedings of Workshop on *Physics and Experiments with Linear e^+e^- Colliders*, eds. R.Orava, P.Eerola and M.Nordberg (World Scientific, Singapore, 1992) p51, and references therein.
10. Proceedings of *Fifth International Workshop on Linear Colliders (LC93)*, October 13-21, 1993, *SLAC report* SLAC-436,p383.
11. E.A.Kushnirenko,proceedings of *The International Workshop on Final Focus and Interaction Regions of Next Generation Linear Colliders*, May 2-6,1992, *SLAC report* SLAC-405,p225.
12. T.Tauchi, K.Yokoya and P.Chen, *Part. Accel.* **41**, 29 (1993).
13. D.Schulte, private communication.
14. T.Tauchi and K.Yokoya, *Phys. Rev.* E **51**, 6119 (1995).
15. D.Schulte, proceedings of LC95 [5], p1419.
16. ,A.Miyamoto, proceedings of *the Third Workshop on JLC* ed. A.Miyamoto, *KEK Proceedings* 92-13, December 1992, p389.
17. P.Chen, T.L.Barklow and M.E.Peskin, *Phys. Rev.* D **49**, 3209 (1994).
18. C.Damerell,these proceedings.
19. Y.Fujii, in proceedings of LCWS93 [4],p782.
20. Y.Sugimoto,*Vertex Detector for JLC* in proceedings of *the 2nd JLC Detector Workshop*, ed. Y.Fujii, February 1-3, 1994, p109.
21. T.Tsukamoto et al.,proceedings of *the 2nd International Symposium on Development of Semiconductor Tracking Detectors*, October 10-13, 1995, to be published in *Nucl. Instr. and Meth.*

22. D.Jackson,these proceedings.
23. I.Nakamura,these proceedings.
24. R.L.Gluckstern, *Nucl. Instrum. Methods* **24**, 381 (1963).
25. N.Khalatyan,these proceedings.
26. K.Ishii,these proceedings.
27. S.Kim, *Nucl. Instrum. Methods* A **360**, 206 (1995).
28. K.löttmann, *DESY* 95-064;
    K.Fujii and T.Omori, *KEK Preprint* 95-127.
29. T.Omori, proceedings of LC95 [5], p606.
30. T.Hirose,these proceedings.
31. T.Okugi, proceedings of LC95 [5], p642.
32. E.G.Bessonov, proceedings of LC95 [5], p594, and references therein.
33. V.V.Parkhomchuk, V.D.Shiltsev and G.V.Stupakov, *Part. Accel.* **46**, 241 (1994) and references therein.
34. S.Kanda, proceedings of LCWS93, p758.
35. S.Takeda(M.Yoshioka),these proceedings.
36. C.Adolphsen,these proceedings.